Does Full-Duplex Double the Capacity of Wireless Networks?

Xiufeng Xie and Xinyu Zhang
University of Wisconsin-Madison
Email: {xiufeng, xyzhang}@ece.wisc.edu

***Abstract*—Full-duplex has emerged as a new communication paradigm and is anticipated to double wireless capacity. Existing studies of full-duplex mainly focused on its PHY layer design, which enables bidirectional transmission between a single pair of nodes. In this paper, we establish an analytical framework to quantify the network-level capacity gain of full-duplex over half-duplex. Our analysis reveals that inter-link interference and spatial reuse substantially reduces full-duplex gain, rendering it well below 2 in common cases. More remarkably, the asymptotic gain approaches 1 when interference range approaches transmission range. Through a comparison between optimal half- and full-duplex MAC algorithms, we find that full-duplex's gain is further reduced when it is applied to CSMA based wireless networks. Our analysis provides important guidelines for designing full-duplex networks. In particular, network-level mechanisms such as spatial reuse and asynchronous contention must be carefully addressed in full-duplex based protocols, in order to translate full-duplex's PHY layer capacity gain into network throughput improvement.**

I. Introduction

Wireless networks have commonly been built on half-duplex radios. A wireless node cannot transmit and receive simultaneously, because the interference generated by outgoing signals can easily overwhelm the incoming signals that are much weaker, so called *self-interference* effect. Yet recent advances in communications technologies showed the feasibility of canceling such self-interference, thus realizing *full-duplex* radios that can transmit and receive packets simultaneously. Substantial research effort has focused on designing full-duplex radios by combining RF and baseband interference cancellation [1], [2], enabling bi-directional transmission between a single pair of nodes. Full-duplex technology is thus anticipated to double wireless capacity without adding extra radios [1], [3], [4].

In practice, however, wireless networks are more sophisticated than a single-link. Real-world wireless networks, such as wireless LANs and mesh networks, are distributed in nature, involving multiple contention domains over large areas, thus entangling both self-interference and inter-link interference. Hence, one may raise an important question: *Does full-duplex double the capacity of such distributed wireless networks?*

This paper establishes a comprehensive analytical framework to quantify the benefits of full-duplex wireless networks. Contrary to widely held beliefs, the analysis leads to a rigorous but negative answer: full-duplex radios cannot double network capacity, even if assuming perfect self-interference cancellation. The key intuition behind this result lies in the *spatial reuse* and *asynchronous contention* effects in wireless networks.

First and foremost, there exists a fundamental tradeoff between spatial reuse and the full-duplex gain. Full-duplex allows a receiver to send packets concurrently, but this extra sender expands the interference region, which would have been reused even by a half-duplex radio. Consider the two-cell WLAN in Fig. 1(a). With half-duplex radios, link TX1→RX1 and TX2→RX2 do not conflict and can be activated concurrently. Whereas full-duplex enables RX1 to transmit simultaneously

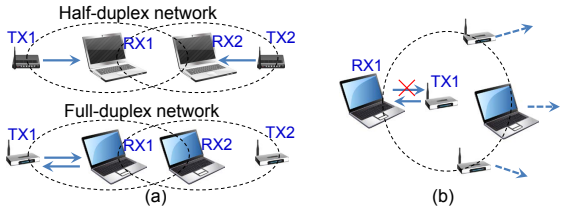

Fig. 1. Spatial reuse and asynchronous contention offsets full-duplex gain. Dotted circles denote interference range. Protocol model [5] is assumed.

with TX1, it suppresses both TX2 (whose receiver RX2 is interfered by RX1) and RX2 (who interferes with receiver RX1). Hence, surprisingly, full-duplex results in the same network capacity as half-duplex in such cases.

Second, to avoid collisions, distributed wireless networks commonly adopt CSMA algorithms that are inherently asynchronous and cannot guarantee a pair of transceivers can access the channel simultaneously to enable full-duplex transmission. As exemplified in Fig. 1(b), two vertices of a link may belong to different contention domains involving independent contenders. When TX1 gains channel access and starts transmission, RX1 may be still in a long backoff stage (as it contends with more interferers) and needs to wait for its turn to transmit.

So, how will these two factors manifest and affect the capacity of large-scale full-duplex wireless networks? Assuming the *protocol model* [5] for channel access, we first analyze the spatial reuse in 1-D random networks and derive the exact capacity gain of full-duplex over half-duplex networks, as a function of Δ, a parameter that governs spatial reuse and reflects the difference between interference range and transmission range. Then, assuming an oracle, synchronized scheduler, we extend the analysis to 2-D networks to obtain an upperbound for the full-duplex capacity gain. Our analysis establishes novel models (*e.g.*, full-duplex exclusive region) that fundamentally differ from those in capacity modeling of half-duplex networks. The analysis proves that under typical settings, *e.g.*, $\Delta = 1$, the capacity gain is only 1.33 in 1-D networks and bounded by 1.58 in 2-D networks. The asymptotic gain approaches 1.28 (*i.e.*, full-duplex improves capacity by only 28%) as $\Delta \to 0$.

Furthermore, we relax the assumption of oracle scheduler with a distributed, asynchronous MAC algorithm that allows a pair of full-duplex transceivers to contend for channel access and transmit packets independently, as if no mutual interference exists. Parameters of the algorithm are controlled by a utility-maximization framework, which can achieve optimal throughput with proportional fairness guarantee. We compare the capacity of this full-duplex MAC with the corresponding utility-optimal half-duplex MAC [6]. Simulation results show that asynchronous contention further reduces the chance of full-duplex transmission in CSMA networks.

Our analysis and simulation implies that it is non-trivial to translate full-duplex' PHY-layer capacity gain to network-level throughput gain. Traditional CSMA-style MAC is no

978-14799-3360-0/14/$31.00 ©2014 IEEE

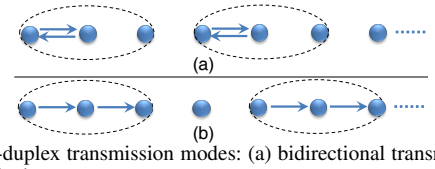

Fig. 2. Full-duplex transmission modes: (a) bidirectional transmission and (b) wormhole relaying.

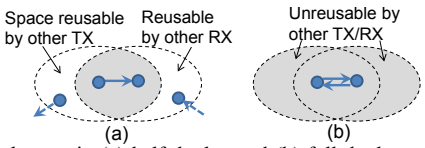

Fig. 3. Spatial reuse in (a) half-duplex and (b) full-duplex networks. Dotted lines denote interference range.

longer the optimal solution for full-duplex radios due to the spatial reuse and asynchronous contention problems. Network designers need to reinvent the medium access protocols to fully exploit the potential of full-duplex communications.

The remainder of this paper is structured as follows. Sec. II introduces the background, model and motivation behind our analysis. Sec. III analyzes the capacity gain of full-duplex over half-duplex networks. Then, Sec. IV quantifies the asynchronous contention effect in full-duplex CSMA networks. Sec. V discusses related work and Sec. VI concludes the paper.

II. Background and Motivation

A. Network model

In this section, we present the essential models and assumptions underlying our analytical framework.

Full-duplex communications. A full-duplex radio can transmit and receive different packets at the same time. Its interference-cancellation hardware and baseband signal processors can effectively isolate the interference from transmitted signals to received ones. In practice, perfect isolation is infeasible due to RF leakage. Even with sophisticated hardware, a full-duplex link can achieve around 1.84 capacity gain compared with a half-duplex link [1]. In this paper, however, we will assume perfect full-duplex radios to isolate the PHY-layer artifacts, and focus on the network-level capacity gain instead.

From a network perspective, full duplex links can operate in two modes [1]. *Bidirectional transmission mode* (Fig. 2(a)) allows a pair of nodes to transmit packets to each other simultaneously. It is applicable to WLANs with uplink/downlink traffic, or multi-hop networks with bidirectional flows. *Wormhole relaying mode* (Fig. 2(b)) enables a receiving node to forward packets to another node simultaneously, thus accelerating data transportation in multi-hop wireless networks. Alternatively, full-duplex radios can send busy-tones while receiving, thus preventing hidden terminals [1]. Such schemes underutilize the capacity as the busy-tone contains no data, and thus they are beyond the scope of this paper.

Topology and interference model. We consider ad-hoc networks where nodes are random uniformly distributed in a region of fixed area, which can be a unit line segment in one dimension, or a unit square in two dimensions. We extend the widely adopted *protocol model* [5] to represent the adjacent link interference in full-duplex networks. Denote X_i as the location of node i. Any transmission from node i to j can be successful *iff* $|X_i - X_j| \leq r$, and $\forall k \neq j$, $|X_k - X_j| > (1+\Delta)r$. Here r and $(1+\Delta)r$ are the transmission range and interference range, respectively. In multi-hop networks, to ensure end-to-end connectivity between any two nodes, r is a function of n, the number of nodes in the network, and must satisfy $r = \Theta(\sqrt{\frac{\log n}{n}})$ [5].

B. Factors affecting the full-duplex gain

Whereas full-duplex has the potential to double the capacity of a single pair of nodes, we identify the following network-level factors which degrade the capacity gain when multiple contending links are entangled.

Spatial reuse. Full-duplex allows a receiver to become an active transmitter simultaneously, but this creates more interference and expands the effective spatial occupation of a pair of nodes, compared with a half-duplex link. As shown in Fig. 3(a), for a half-duplex link, the receiver is passive and another receiver of a nearby link can be placed close to it without mutual interference. Similarly, transmitters of two links can be placed close by. Hence, within the union of the transmitter and receiver's interference range, there exists a sizable fraction of space that can be reused by nodes of other links. In contrast, if full-duplex radios are employed and every node is a transmitter and receiver, then no space is reusable by other nodes (Fig. 3(b)). In other words, full-duplex cannot double the number of concurrent transmissions in a network. Therefore, *despite the doubling of single-link capacity, full-duplex sacrifices spatial reuse and consequently, may not double the network-wide capacity.*

Asynchronous contention. Wireless LANs and multi-hop networks commonly adopt the asynchronous CSMA based contention algorithms. Two vertices of a link are separated in space, and may be contending with different set of neighbors. Hence, they may have different channel status (idle/busy) at any time instance. Transitions between channel status are also inherently asynchronous due to unpredictable dynamics in each neighborhood. Even when both are idle, the two nodes cannot transmit immediately — they must respect the CSMA backoff mechanism and wait for their backoff counters to expire in order to avoid collision. And again, the backoff counters are asynchronous — a node with more contenders tends to have a larger backoff counter, and needs to wait for a longer idle period before transmission.

However, to maximize the full-duplex gain, a pair of nodes must be able to synchronize their transmissions, *i.e.*, ensuring both channels are idle and backoff counters fire at the same time. Yet such synchronization requires both nodes to be aware of each other's channel status in each time slot, which is infeasible in practice. Therefore, *when applied to real-world CSMA networks, full-duplex radios need to inevitably respect the asynchronous contention, which reduces the chance of full-duplex transmissions and the capacity gain.*

Other factors. Different transmission modes may affect full-duplex gain differently, as exemplified in Fig. 2. Assume $\Delta = 0$, *i.e.*, interference range equals transmission range. When wormhole relaying is applied for a single linear flow, the normalized end-to-end throughput can be $\frac{1}{2}$ (for every 4 hops, there can be 2 transmitters), in contrast to $\frac{1}{3}$ for half-duplex

nodes. Hence, wormhole relaying leads to a capacity gain of 1.5. On the other hand, bidirectional transmission mode can be applied to bi-directional flows, increasing the capacity to $\frac{2}{3}$, potentially doubling the capacity of two linear flows.

The case is different when Δ varies and changes the spatial reuse accordingly. For instance, if $\Delta = 1$, wormhole relaying becomes infeasible as the first transmitter interferes the second transmitter's receiver, although bidirectional transmission still helps in improving end-to-end throughput of multiple flows. Therefore, *both the transmission mode and interference range parameter Δ have significant impacts on the full-duplex gain.*

In what follows, we rigorously analyze the capacity gain of full-duplex over half-duplex networks by incorporating the above factors. Sec. III bounds the capacity gain assuming synchronized full-duplex transmissions. Sec. IV further relaxes the assumption with an asynchronous channel contention model.

III. Full-duplex Gain: Asymptotic Analysis

In this section, we characterize the asymptotic capacity gain of full-duplex over half-duplex ad hoc networks, as the number of nodes $n \to \infty$. Each node is a source node and its destination is randomly chosen. Network capacity λ is conventionally defined as the maximum data rate that can be supported between every source–destination pair [5].

Let D denote the average distance between a source node and its destination, d the average distance of a hop, then the average number of hops in each end-to-end flow is D/d, and each flow requires a MAC-layer throughput of $\lambda D/d$. Since there are n flows in this network, total demand for MAC-layer throughput is $n\lambda D/d$.

Let $N(d)$ denote the maximum number of simultaneous transmission links. It is a function of hop distance d, which affects the spatial reuse between links. Suppose the data rate of any transmission link is W, then the maximum supportable MAC-layer throughput is $WN(d)$. The demand for MAC-layer throughput cannot exceed the supportable amount, thus:

$$\lambda = \frac{W}{nD} \max_{0<d\le r} (dN(d)) \tag{1}$$

A. 1-D Chain Network

In this section, we first derive tight capacity bounds for one-dimensional full-duplex and half-duplex networks in Lemma 1 and Lemma 2, respectively. Then we characterize the full-duplex capacity gain in Theorem 1.

Similar to the model in [7], we assume all nodes are uniformly and randomly distributed within a 1-D network of unit length. Then we partition the unit length region into a set of bins. Length of each bin is $l(n) = K\frac{\log(n)}{n}$, K is chosen to ensure that transmission range $r \gg l(n)$, so that a node in one bin can always reach any node in an adjacent bin. As proved in [8], as $n \to \infty$, there is at least one node in each bin with high probability.

Lemma 1 *The per-flow capacity of a 1-D full-duplex random network is*

$$\lambda_F = \frac{W}{nD} \cdot \frac{2}{2+\Delta} \tag{2}$$

Proof: We treat the two full-duplex modes separately.

(i) Bidirectional transmission mode. Consider a full-duplex bidirectional transmission pair $A \leftrightarrow B$ with link distance d. As shown in Fig. 4, to avoid interference, the distance between A and the right-most node of any transmission pair left to $A \leftrightarrow B$ must be larger than $(1+\Delta)r$.

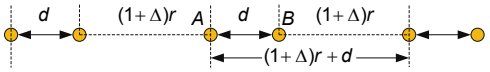

Fig. 4. Exclusive region for 1-D bidirectional transmission mode.

Therefore, each transmission pair must at least occupy a line segment of length $(1+\Delta)r + d$. By dividing the network size (unit length) by this minimum length, maximum number of simultaneous transmission pairs is upper bounded by $\frac{1}{(1+\Delta)r+d}$.

In bidirectional mode, each transmission pair can support data rate of $2W$. Combining Eq. (1), we have the upperbound of per-flow capacity in bidirectional mode:

$$\lambda_B \le \frac{W}{nD} \cdot \max_{0<d\le r} \frac{2d}{(1+\Delta)r + d} \tag{3}$$

From Eq. (3), we observe that when $d = r$, the network has the maximum throughput, which means the upperbound has the same form as Eq. (2) in Lemma 1.

For the capacity lowerbound, we constructively schedule flows following the schedule pattern in Fig.4. Note that it is a random network, and distance between any two nodes will tolerate a small disturbance of twice the bin size. Thus each transmission will travel a distance in the interval of $[r-2l, r]$, and the distance between two adjacent transmission pairs should be in the interval of $[(1+\Delta)r - 2l, (1+\Delta)r]$. Similar to [7], in order to make the disturbance negligible, we can choose a proper bin size $l(n)$ which ensures transmission range $r \gg l(n)$, let $K_2 = r/l(n)$, K_2 should be a large constant, then the lowerbound becomes:

$$\lambda_B \ge \frac{W}{nD} \frac{2(r - \frac{2}{K_2}r)}{(1+\Delta)r + (r - \frac{2}{K_2}r)} \approx \frac{W}{nD} \cdot \frac{2}{2+\Delta}$$

Since this constructive lowerbound equals the upperbound, we have the per-flow capacity in Lemma 1.

(ii) Wormhole relaying mode. A wormhole relaying triple $A \to R \to B$ consists of 3 nodes: a half-duplex transmitter A, a full-duplex relay node R, and a half-duplex receiver B. Consider two adjacent wormhole relaying triples $A_1 \to R_1 \to B_1$ and $A_2 \to R_2 \to B_2$ as shown in Fig. 5. The link distance of $A_1 \to R_1$ and $R_1 \to B_1$ equals d. To maximize spatial reuse (*i.e.*, packing the maximum number of links inside the unit length network), receivers B_1 and B_2 (or equivalently transmitters A_1 and A_2) must be placed adjacent to each other. In addition, the distance between relay R_1 and receiver B_2 must be larger than the interference range $(1+\Delta)r$.

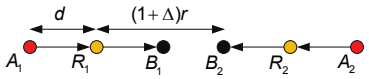

Fig. 5. Exclusive region for 1-D wormhole relaying mode.

Consequently, there can be at most one triple within any line segment of length $(1+\Delta)r + d$. Since each triple contains two transmission links, every two links must occupy a line segment of minimum length $(1+\Delta)r + d$, which is the same as in the bidirectional transmission mode. Then with a similar derivation

as above, we can obtain the same capacity upperbound and lowerbound, which concludes the proof for Lemma 1. □

We note that for each wormhole relaying triple $A \to R \to B$, the distance between A and B must be larger than $(1+\Delta)r$ to avoid interference, *i.e.*, $2d > (1+\Delta)r$. As capacity is maximized when $d = r$, this implies wormhole relaying can achieve the same capacity as bidirectional transmission only if $0 \le \Delta < 1$, which is also the practical range for Δ [9].

Lemma 2 *The per-flow capacity of a 1-D half-duplex random network is*

$$\lambda_H = \frac{W}{nD} \cdot \frac{1}{1+\Delta} \tag{4}$$

Proof: For half-duplex radios, the distance between RX and TX from different transmission pairs must be larger than $(1+\Delta)r$. Therefore, the minimum length of line segment occupied by each transmission pair is $L_H = (1+\Delta)r$, as shown in Fig. 6.

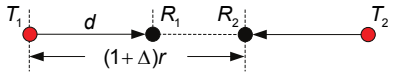

Fig. 6. Exclusive region for a 1-D half-duplex network.

Since each half-duplex transmission pair only contains one transmission link, the maximum number of transmission links that can be accommodated in the unit length network is: $\frac{1}{(1+\Delta)r}$. Combining with Eq. (1), we have the capacity upperbound of the half-duplex scheme:

$$\lambda_H \le \frac{W}{nD} \max_{0<d\le r} \frac{d}{(1+\Delta)r} \tag{5}$$

When $d = r$, λ_H achieves its maximum, which leads to the upperbound for Eq. (4) in Lemma 2.

With a similar method as in the full-duplex case, we can construct the half-duplex lowerbound:

$$\lambda_H \ge \frac{W}{nD} \frac{r - \frac{2}{K_2}r}{(1+\Delta)r} \approx \frac{W}{nD} \cdot \frac{1}{1+\Delta} \tag{6}$$

which, combined with the upperbound, leads to Lemma 2. □

Based on Lemma 1 and Lemma 2, we can obtain the full-duplex capacity gain of a 1-D random network.

Theorem 1 *The full-duplex gain of a 1-D random network is*

$$G_1 = \frac{\lambda_F}{\lambda_H} = \frac{2+2\Delta}{2+\Delta} = 1 + \frac{\Delta}{2+\Delta} \tag{7}$$

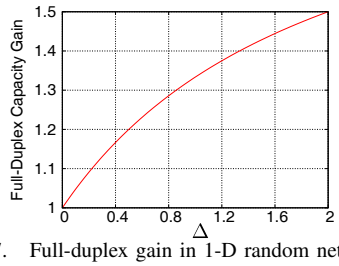

Fig. 7. Full-duplex gain in 1-D random networks.

Implication: Fig. 7 plots the full-duplex gain under varying Δ. When $\Delta = 0$, the asymptotic gain is 1, even though it can be larger than 1 in certain finite cases (Sec. II-B). The gain increases with Δ and approaches 2 as $\Delta \to \infty$, when the entire network falls in one contention domain. However, in the common case of $0 \le \Delta \le 1$, the gain is no larger than 1.33, far from doubling network capacity.

B. Full-Duplex Gain in 2-D Networks

In this section, we bound the full-duplex capacity gain by comparing capacity upperbound of full-duplex networks and lowerbound of half-duplex networks.

1) Exclusive region for full-duplex nodes: We extend the classic approach [5] of deriving capacity upperbound to the full-duplex case. Network capacity is proportional to the number of simultaneous transmission links that can be accommodated. Thus an upperbound can be obtained by dividing total network area by a link's exclusive region, the area no other active transmitter or receiver can reuse.

We assume all links operate in the bidirectional transmission mode. A node is both TX and RX at the same time, hence the distance between any two nodes (except those belonging to the same bidirectional link) must be larger than interference range $(1+\Delta)r$. Based on this observation, we define the exclusive region in Fig. 8, which is the union of two circles with radius $R = \frac{(1+\Delta)r}{2}$.

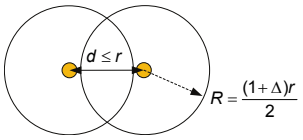

Fig. 8. Exclusive region for a full-duplex bidirectional transmission pair.

Under this definition, if two exclusive regions do not overlap, the distance between their nodes will be larger than $(1+\Delta)r = 2R$, *i.e.*, they do not interfere with each other. Conversely, if any two exclusive regions overlap, the minimum distance between two nodes from each region will be smaller than $(1+\Delta)r$, resulting in interference. Therefore, *the sufficient and necessary condition for interference-free transmission in bidirectional mode is that no two exclusive regions overlap.*

2) Capacity upperbound of 2-D full-duplex random networks: Consider a 2-D random network where n full-duplex nodes are distributed uniformly within a 1×1 unit square. Its capacity upperbound can be characterized as follows:

Theorem 2 *The per-flow throughput capacity λ_F of 2-D full-duplex random network is upper bounded by*

$$\lambda_F < \frac{W}{nD(1+\Delta)^2 r} \cdot \frac{4}{\pi - \arccos(\frac{1}{1+\Delta}) + \frac{\sqrt{\Delta^2+2\Delta}}{(1+\Delta)^2}}$$

for large n.

Proof: First, we can derive the area S_F of the exclusive region defined above, with $R = \frac{(1+\Delta)r}{2}$:

$$S_F = 2\pi R^2 - 2(R^2 \arccos(\frac{d}{2R}) - \frac{d}{2}\sqrt{R^2 - (\frac{d}{2})^2})$$

By dividing the network area by S_F, we can derive the upperbound of the maximum number of simultaneous transmission pairs. In the bidirectional transmission mode, one transmission pair contains two transmission links, thus the maximum number of simultaneous transmission links is $N_F = 2/S_F$.

Then from Eq. (1), we can derive the upperbound of per-flow capacity of 2-D full-duplex random networks under a given d:

$$\frac{2W}{nDR} \max_{0<d\le r} \left(\frac{\frac{d}{2R}}{\pi - \arccos(\frac{d}{2R}) + \frac{d}{2R}\sqrt{1-(\frac{d}{2R})^2}}\right) \tag{8}$$

Then we need to find the optimal value of d which leads to the maximum per-flow throughput λ_F. Let $x = d/2R$, $C = \frac{2W}{nDr}$, and $\lambda_F = f(x)$:

$$f(x) = C\frac{x}{\pi - \arccos(x) + x\sqrt{1-x^2}} \tag{9}$$

The first order derivative of $f(x)$ is:

$$\frac{\mathrm{d}f(x)}{\mathrm{d}x} = C\frac{\pi - \arccos(x) + \frac{x+x^2(2-x)}{\sqrt{1-x^2}}}{\left(\pi - \arccos(x) + x\sqrt{1-x^2}\right)^2} \tag{10}$$

Since $x = d/2R$, $0 < x < 1$, we have $\frac{\mathrm{d}f(x)}{\mathrm{d}x} > 0$. Therefore, $f(x)$ is a monotonic increasing function of x when $0 < x < 1$. Because $x = d/2R$ and $d \le r$, the network achieves maximum per-flow throughput when $d = r$. With this observation and Eq. (8), we can obtain the network capacity in Theorem 2. □

Based on Theorem 2, combined with the connectivity requirement that $r = \Theta(\sqrt{\log(n)/n})$, we can obtain a capacity scaling law for random full-duplex networks:

Corollary 1 *For a random full-duplex network, $\lambda_F(n) = O(1/\sqrt{n\log(n)})$ as $n \to \infty$*

This implies that full-duplex may improve network capacity by at most a multiplication factor. Its asymptotic capacity remains the same as that of a half-duplex network [5].

3) Full-duplex gain in 2-D regular networks: To make a fair comparison, ideally full-duplex should be evaluated against half-duplex capacity in the same topology. However, the exact capacity of a 2-D random network is always difficult to obtain. Therefore we first focus on a regular lattice network: nodes are located at junction points, and the distance between adjacent junction points equals transmission range r. With similar method for the 2-D random network, we can derive the full-duplex capacity upperbound for 2-D lattice network:

Lemma 3 *The per-flow throughput capacity λ_F of 2-D full-duplex regular lattice network is upper bounded by*

$$\lambda_F < \frac{2W}{nDr} \cdot \frac{1}{\left\lceil \frac{(1+\Delta)^2(\pi - \arccos\frac{1}{(1+\Delta)}) + \sqrt{\Delta^2+2\Delta}}{2} \right\rceil}$$

for large n.

Proof: In a lattice network, the exclusive region should contain a set of square cells with side length r. Given the necessary and sufficient condition for interference-free transmission (Sec. III-B1), we can find the area of the exclusive region S_F^R in such a network: $S_F^R = \left\lceil \frac{S_F}{r^2} \right\rceil r^2$. Since the link distance d can only be r, we can derive the full-duplex upperbound for lattice network similarly to the random network case and obtain Lemma 3. □

In addition, we can obtain a lowerbound of half-duplex per-flow capacity in lattice networks by constructing an achievable schedule.

Lemma 4 *The per-flow throughput capacity λ_H of 2-D half-duplex regular lattice network is lower bounded by*

$$\lambda_H > \frac{W}{nDr} \cdot \frac{1}{\left\lceil \max(1, \sqrt{\Delta^2+2\Delta})(1+\Delta) \right\rceil} \tag{11}$$

for large n.

Proof: A 2-D regular network is equivalent to multiple 1-D regular networks placed in parallel. To construct a feasible schedule, we divide time into slots: even slots are used to transmit data horizontally, and odd ones for vertical transmission. Thus all nodes in the network can be ensured the same chance to send data. Fig. 9 illustrates a snapshot of the constructed schedule.

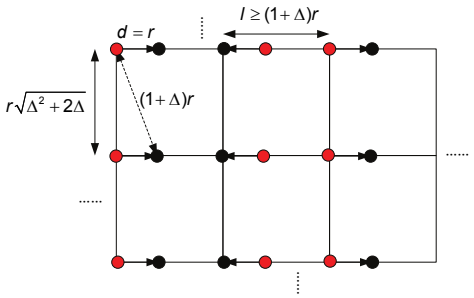

Fig. 9. Half-duplex capacity lowerbound.

To avoid interference, the distance between parallel flows cannot be smaller than $r\sqrt{\Delta^2+2\Delta}$. Meanwhile, in the lattice network, the distance between two nodes cannot be smaller r. Therefore the minimum distance between parallel flows should be $\max(r, r\sqrt{\Delta^2+2\Delta})$, and there can be only one transmission in each rectangle block of side lengths $(1+\Delta)r$ and $\max(r, r\sqrt{\Delta^2+2\Delta})$, thus the space occupied by each transmission link is:

$$S_H = \left\lceil \frac{\max(1, \sqrt{\Delta^2+2\Delta})(1+\Delta)r^2}{r^2} \right\rceil r^2 \tag{12}$$

By dividing the unit square area by area of the space occupied by each transmission link, we can obtain the supportable number of simultaneous transmission links:

$$N_H \ge \left(\left\lceil \max(1, \sqrt{\Delta^2+2\Delta})(1+\Delta) \right\rceil r^2 \right)^{-1} \tag{13}$$

From Eqs. (13) and (1) we obtain the per-flow capacity lowerbound λ_H of 2-D lattice network in Lemma 4. □

Finally, by comparing full-duplex capacity upperbound (Lemma 3) and half-duplex lowerbound (Lemma 4), we can bound the full-duplex capacity gain for 2-D lattice networks.

Theorem 3 *For a 2-D regular lattice network, full-duplex capacity gain of is upper bounded by*

$$G_{2L} = \frac{\lambda_F}{\lambda_H} < \frac{2\left\lceil \max(1, \sqrt{\Delta^2+2\Delta})(1+\Delta) \right\rceil}{\left\lceil \frac{(1+\Delta)^2(\pi - \arccos\frac{1}{(1+\Delta)}) + \sqrt{\Delta^2+2\Delta}}{2} \right\rceil}$$

This result implies that the upperbound of full-duplex gain G_{2L} is determined only by Δ, and unrelated to number of nodes n or transmission range r. Fig. 10 plots the relationship between G_{2L} and Δ.

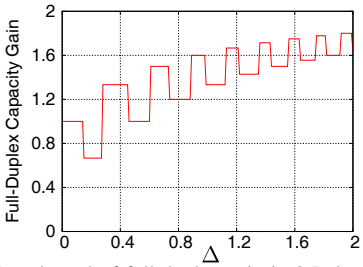

Fig. 10. Upperbound of full-duplex gain in 2-D lattice networks.

Implication: In general, G_{2L} increases with Δ, because for larger Δ, the fraction of space reusable by neighboring links

decreases in half-duplex networks (as illustrated in Fig 11), and thus full-duplex advantage is more prominent. However, G_{2L} is always below 2 in the practical range of $0 \leq \Delta \leq 1$, which matches our intuition in Sec. II. Note that the fluctuation of G_{2L} is caused by the ceiling functions in Theorem 3. In certain cases, G_{2L} can fall below 1 when the spatial reuse effect overwhelms the benefit of full-duplex transmission.

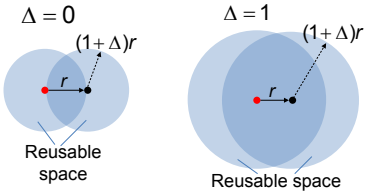

Fig. 11. For half-duplex, with larger Δ, a smaller fraction of space can be reused by neighboring links.

4) Full-duplex gain in 2-D random networks: In this section, we first construct a capacity lowerbound for 2-D half-duplex random networks, and then compare it with the upperbound in Theorem 2 in order to bound the full-duplex capacity gain.

Lemma 5 *For large n, the throughput capacity λ_H of 2-D half-duplex random network is lower bounded by*

$$\lambda_H \geq \frac{W}{nD(1+\Delta)^2 r} \tag{14}$$

Proof: We can partition the network into regular cells (Fig. 12(a)), each being a square with side length $l(n) = K\sqrt{\frac{\log(n)}{n}}, K > 1$. As proved in [8], for large n with high probability there is at least one node in each cell.

Then we can construct a schedule by expanding the 1-D schedule in Lemma 2, as illustrated in Fig. 12(b). We schedule nodes along a row (or column) of cells. Multiple 1-D schedules are placed parallelly, and the distance between them must be larger than $(1+\Delta)r$. Time is slotted to schedule transmissions along rows and columns, similar to the proof for Lemma 4.

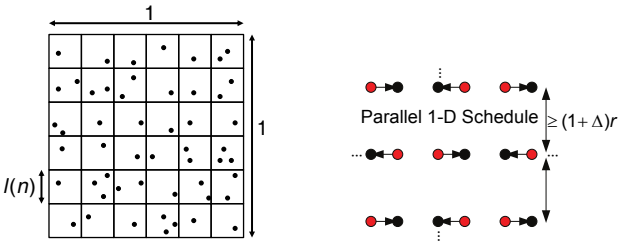

(a) Cell partition (b) Lowerbound construction

Fig. 12. Constructing a capacity lowerbound for 2-D random networks.

As nodes are random uniformly distributed, the distance between parallel 1-D schedules has a small disturbance of twice the side length of a cell, and falls in the range of $[(1+\Delta)r, (1+\Delta)r + 2l(n)]$. In order to cancel the small disturbance caused by topology randomness, we can choose a large transmission range $r = K_2 l(n)$, where K_2 is a large constant. Then the disturbance is negligible, and the number of simultaneous parallel 1-D schedules is lower bounded by:

$$\frac{1}{(1+\Delta)r(n) + \frac{2r(n)}{K_2}} \approx \frac{1}{(1+\Delta)r(n)} \tag{15}$$

Combining Eq. (15) with the capacity of 1-D half-duplex network in Lemma 2, we can derive the capacity lowerbound λ_H in Lemma 4. □

From Lemma 5 we can also observe that this constructive lowerbound follows the scaling law in [5]. By synthesizing Theorem 2 and Lemma 5, we can easily prove:

Theorem 4 *The full-duplex capacity gain of a 2-D random network is upper bounded by*

$$G_{2R} = \frac{\lambda_F}{\lambda_H} < \frac{4}{\pi - \arccos(\frac{1}{1+\Delta}) + \frac{\sqrt{\Delta^2+2\Delta}}{(1+\Delta)^2}} \tag{16}$$

for large n.

Implication: Similar to regular networks, the upperbound of full-duplex gain in random network depends on Δ. Fig. 13 plots G_{2R} as Δ varies. Under a typical setting of $\Delta = 1$, G_{2R} is only 1.58, and approaches 1.28 as $\Delta \to 0$, *i.e.*, transmission range approaches interference range. Note that in practical wireless networks, Δ can be very close to 0, especially for links with low bit-rate (and thus longer transmission range) [9].

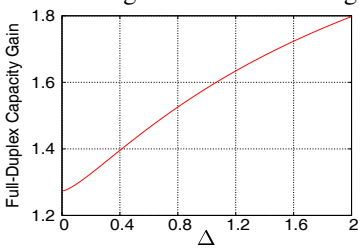

Fig. 13. Upperbound of full-duplex gain in 2-D random networks.

IV. Full-duplex Gain Under Asynchronous Contention

In this section, we introduce a full-duplex MAC that conforms to the asynchronous contention mechanism of practical CSMA networks. We first describe the protocol operations, and then build a distributed optimization framework that adapts the operations to achieve optimal network throughput. We will compare the capacity of this full-duplex MAC with an optimal half-duplex MAC.

A. Full-duplex MAC: model and protocol

The proposed full-duplex MAC retains primitive operations (*e.g.*, carrier sensing and backoff) of the widely-adopted 802.11 MAC, but with two features specific to full-duplex: *(i)* While in receiving mode, a receiver can continue sensing its channel status [10]. It marks a busy channel if the channel is occupied simultaneously by nodes *other than its own transmitter. (ii)* While in receiving mode, a receiver can transmit back to the sender if it senses an idle channel and finishes backoff. Here we only consider the bidirectional transmission mode.

Fig. 14 illustrates a typical channel contention procedure for the full-duplex MAC. As the transmitter and receiver's MAC operations cannot be synchronized, they need to contend for channel access independently. Full-duplex opportunity occurs only when their transmissions overlap. The contention procedure is similar to 802.11 CSMA, except that each pair of transmitter/receiver are aware that they do not interfere with each other. Specifically, before transmission, a node needs to sense the channel for a DIFS duration [11]. After sensing an

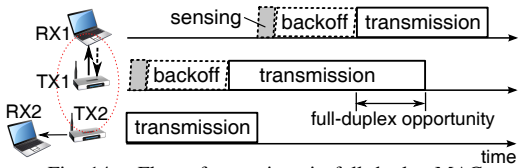

Fig. 14. Flow of operations in full-duplex MAC.

idle channel, it starts backoff and waits for an additional idle duration of B time slots, with B randomly chosen from $[0, CW]$. It freezes the backoff if the channel becomes busy again, and resumes otherwise. Upon completing the backoff, it begins transmission immediately. *CW*, the *backoff window size*, is reset to $CW_{\min}$ upon each successful transmission, and doubled upon failure until reaching a maximum value of $CW_{\max}$ [11].

To ensure a *fair comparison* between half-duplex and full-duplex network *capacity*, we assume perfect carrier sensing for both, *i.e.*, a transmitter is aware of all other transmitters that can interfere with its receiver. This complies with the protocol model, which assumes no hidden terminal and exposed terminal problems.

In practical half-duplex networks, hidden terminals can be significantly reduced using the RTS/CTS message exchange before data transmission [9]. Exposed terminal problem can be solved approximately by building a conflict graph offline [12], which specifies the interference relation between links. Similar mechanisms can be applied to full-duplex networks. To realize RTS/CTS for full-duplex bidirectional transmission, an active transmitter should be able to decode RTS requests from the receiver. If the transmitter is not disrupted by strong interferers to the RX→TX link, then it can temporarily suspend its data transmission, and feeds back a CTS packet to the RX instead. RX then starts transmission and TX resumes its transmission. To combat the exposed terminal, an offline conflict graph can be used, similarly to half-duplex networks [12]. Even if two transmitters can sense each other, they can still send packets concurrently if their mutual interference is much weaker compared with the signal strength at the receiver of each.

B. Utility-optimal full-duplex MAC: optimization formulation and distributed solution

We consider the problem of optimizing MAC-layer throughput capacity for a network containing a given set Γ of links that run the above asynchronous contention protocol. Every link is a single-hop connection and has a counterpart of reverse direction, thus $|\Gamma|$ is an even number and the number of nodes equals $|\Gamma|$. Denote $\mathcal{S}$ as the set of independent sets (each is a subset of non-interfering links within Γ). In full-duplex mode, a link and its reverse counterpart can belong to the same independent set. At any time instance, the set of transmitting links correspond to one independent set. A MAC scheduling algorithm can be characterized by π_s, the fraction of time each independent set $s \in \mathcal{S}$ is scheduled. Each link e may appear in multiple independent sets, and its throughput ρ_e equals the sum time of all these sets. Our objective is to map the above asynchronous contention protocol to such a scheduling algorithm, and optimize its parameters to maximize network throughput subject to a fairness constraint. This is equivalent to a utility optimization problem:

$$\max \quad \sum_{e\in\Gamma} U(\rho_e) \tag{17}$$

$$s.t. \quad \rho_e \le \sum_{e\in s, s\in\mathcal{S}} \pi_s, \forall e \in \Gamma \tag{18}$$

$$\sum_{s\in\mathcal{S}} \pi_s = 1 \tag{19}$$

When $U(\rho_e) = \log(\rho_e)$, the objective is proven to achieve optimal throughput with proportional fairness guarantee [6] among $\forall e \in \Gamma$. Similar to half-duplex networks, finding the optimal schedule is an intractable problem. However, the problem can be approximately solved by replacing the objective function with:

$$\max \quad V\sum_{e\in\Gamma} U(\rho_e) - \sum_{s\in\mathcal{S}} \pi_s \log(\pi_s) \tag{20}$$

where V is a positive constant. Because $-\sum_{s\in\mathcal{S}} \pi_s \log(\pi_s) \le \sum_{s\in\mathcal{S}} |\mathcal{S}|^{-1} \log(|\mathcal{S}|) = \log(|\mathcal{S}|)$, it can be easily seen that the approximation deviates from the optimum by at most $\frac{\log(|\mathcal{S}|)}{V}$, which is negligible for large V. In what follows, we derive a distributed asynchronous MAC by solving the approximated optimization problem, using a subgradient method in a similar manner to the utility-optimal half-duplex MAC in [6].

The above approximated optimization (20) can be easily proven to be convex, and its Lagrangian is:

$$L(\boldsymbol{\rho}, \boldsymbol{\pi}, \boldsymbol{q}, \beta) = V\sum_{e\in\Gamma} U(\rho_e) - \sum_{s\in\mathcal{S}} \pi_s \log(\pi_s) + q_e \sum_{e\in s, s\in\mathcal{S}} \pi_s - q_e\rho_e - \beta(\sum_{s\in\mathcal{S}} \pi_s - 1) \tag{21}$$

with dual variables q_e and β. By solving the KKT condition following a similar procedure to [6], we can obtain the optimal values of β and π_s as:

$$\beta^* = \log\Big(\sum_{s\in\mathcal{S}} \exp(\sum_{e\in s} q_e)\Big) - 1 \tag{22}$$

$$\pi_s^* = \frac{\Pi_e \exp(q_e)}{\sum_{s\in\mathcal{S}} \Pi_{e:e\in s} \exp(q_e)} \tag{23}$$

In addition, a subgradient of the dual variable q_e is:

$$\dot{q_e} = \Big[(V/q_e) - \sum_{s:s\in\mathcal{S}, e\in s} \pi_s\Big]^{Q_r} \tag{24}$$

where Q_r denotes the projection to $[q_{\min}, q_{\max}]$, the range of q_e. The dual variable q_e can be interpreted as a virtual queue for each link. The subgradient adaptation (24) converges to the optimal q_e for the utility optimization problem (20) [6]. More importantly, it is fully distributed for each link e. Suppose time is divided into frames, each starting when a packet is generated or successfully transmitted. In each frame, a link e only needs to observe the number of successful transmissions (which accounts for the term $\sum_{s:s\in\mathcal{S}, e\in s} \pi_s$), and adapt q_e following (24).

It has been proven that, by running a CSMA protocol with packet generation rate p_e for each link e and exponentially-distributed packet duration with mean μ_e, the stationary distribution of π_s is [13]:

$$\pi_s = \frac{\Pi_e p_e \mu_e}{\sum_{s\in\mathcal{S}} \Pi_{e:e\in s} p_e \mu_e} \tag{25}$$

Algorithm 1 Utility-maximizing full-duplex CSMA.

1. For each time frame, generate a packet with probability p_e and exponentially distributed duration (in terms of the number of slots) with mean μ_e.
2. Continuously run the full-duplex CSMA/CA protocol in Sec. IV-A.
3. **if** transmission completes or new packet arrives **then**
4. Update q_e according to:
5. $q_e \leftarrow q_e + \alpha(V/q_e - K_e)^{Q_r}$
6. Set p_e and μ_e according to $p_e\mu_e = \exp(q_e)$ **endif**
7. **goto** 1.

Thus, to achieve optimal utility using CSMA, it is sufficient to adapt q_e and set p_e and μ_e in each time frame such that $\exp(q_e) = p_e\mu_e$ (c.f., Eq. (23)). With this observation, we obtain the adaptive CSMA Algorithm 1 for each full-duplex link. Here α is a small step size, and K_e the number of served packets in the time frame. The algorithm essentially controls the rate of each link in order to achieve the optimal utility when combined with the underlying full-duplex CSMA contention algorithm that avoids collision. Note that Q_r can be defined according to practical values of μ_e and λ_e in 802.11 networks.

C. Full-duplex gain: experimental simulation

We compare the achievable capacity of the above full-duplex CSMA algorithm with a utility-optimal half-duplex algorithm [6] which is derived from an optimization framework similar to (17), but does not allow a receiver to sense or transmit while receiving packets. Both algorithms are implemented in a C++ based discrete event simulator with MAC/PHY parameters (*e.g.*, time slot, CW range) consistent with 802.11g [6]. All links are assumed to have a capacity of 6Mbps without rate adaptation. By default Δ equals 1. We consider two types of topologies: *(i)* Multi-cell WLANs with varying link distance and bipolar Poisson distribution of nodes [14]. APs' locations follow Poisson distribution with a given density, and each AP is paired with a client in a random direction with a given distance d. *(ii)* Ad-hoc networks with random uniform distribution of node locations in a fixed 2-D area. Given node density (average number of neighbors within transmission range), the topology generator keeps random trials until obtaining a topology where all nodes are connected. Without loss of generality, each node is paired with one neighbor for bidirectional transmission, and MAC-layer capacity (total throughput of all links) is used as performance metric.

Effects of asynchronous contention. We study the asynchronous contention effect (Fig. 1(b)) by simulating the above utility-optimal CSMA in an ad-hoc network with 100 nodes, density 6. Fig. 15(a) shows the distribution of the number of concurrent transmitters over 10^5 time slots. Due to asynchronous contention, bidirectional links often cannot be scheduled concurrently. Coupled with the effects of spatial reuse, full-duplex results in only 1.47× average gain over half-duplex mode.

One may argue that the contention overhead can offset the improvement of concurrency owing to full-duplex. Fig. 15(b) plots the results of an oracle, round-based scheduler with no contention overhead. In each slot, it randomly selects transmitters who do not interfere those links already selected, until no more transmitters can be selected. This scheduler better leverages the full-duplex advantage and improves concurrency, but the capacity gain is still far below 2, as transmitters are still selected asynchronously, and the effect of spatial reuse persists.

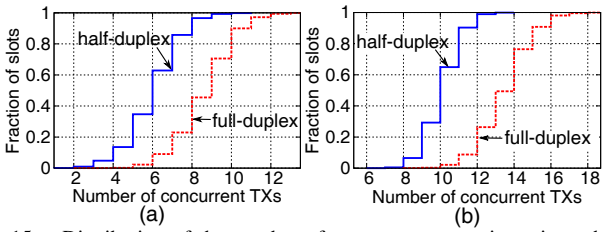

Fig. 15. Distribution of the number of concurrent transmitters in each slot: (a) utility-optimal, distributed, asynchronous CSMA; (b) oracle scheduler that randomly picks transmitters (no contention overhead).

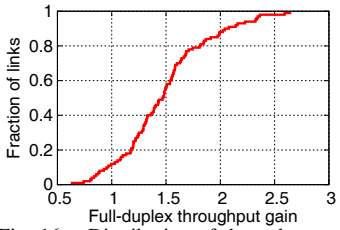

Fig. 16. Distribution of throughput gain.

Capacity gain. Fig. 16 plots the distribution of throughput gain over all 100 links. The utility-optimal, proportionally fair scheduler allocates throughput quite differently for half- and full-duplex networks. Whereas some links receive 2.5× throughput gain, others' throughput may be reduced when using full-duplex. The average throughput gain of all links is 1.46. With respect to the Jain's fairness index [6], half- and full-duplex has a fairness index of 0.58 and 0.56, respectively, which are comparable. Overall, full-duplex provides certain capacity gain without noticeable sacrifice of fairness, but again, the gain is well below 2.

Effects of Δ. Our prior analysis identifies Δ, the excess of interference range over transmission range, as a key parameter governing the full-duplex gain. Fig. 17 plots the mean throughput gain under varying Δ (error bars show the *std.* over 100 random topologies). Consistent with our theoretical analysis, the gain increases as Δ increases. But under practical settings, *e.g.*, $\Delta \leq 1$, the gain is far below 2, and is below the theoretical upperbound predicted in Sec. III-B. This essentially verifies our analytical models, and shows the asynchronous contention further offsets the full-duplex gain in practical, large-scale wireless networks.

Effects of traffic locality in WLANs. In multi-cell wireless LANs, a client can arbitrarily approach the AP, thus confining the transmissions to a local area and reducing spatial reuse advantage of half-duplex networks. Fig. 18 evaluates this effect by varying the AP-client distance in a 50-cell network. When the link distance (normalized *w.r.t.* transmission range) is close to 0, half-duplex networks cannot leverage the spatial reuse advantage. Full-duplex opportunities abound and rise the capacity gain close to 2. However, in the common cases with link

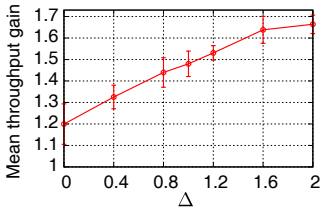

Fig. 17. Effect of Δ in ad-hoc networks.

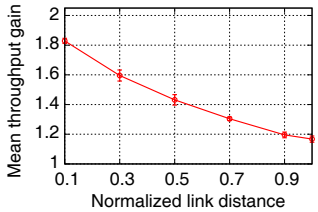

Fig. 18. Full-duplex gain in multi-cell WLANs.

distance above 0.3, the gain is still far below 2 and decreases as link distance increases to 1. Therefore, *full-duplex gain can be prominent in multi-cell WLANs, but only if the AP-client distance is much smaller compared with the transmission range.*

V. Related Work

Full-duplex technology has already been proposed in broadband cellular networks (*e.g.*, WiMax) to facilitate the *frequency-devision mode*. Cellular base stations' transmitting and receiving radios can operate simultaneously in two adjacent frequency bands, and a special hardware filter called duplexer is used to mitigate leakage interference. However, owing to lower cost and better support for asymmetric uplink/downlink traffic, half-duplex time-devision mode is deployed in most cellular networks [15]. Recently, Choi *et al.* [1] realized single-channel full-duplex through delicate antenna placement and self-interference cancellation, which inspired substantial work (*e.g.*, [2], [16], [17]). Research along this direction mainly targets the design and implementation of full-duplex PHY layer. The implication for higher-layer (*e.g.*, multi-hop routing [18], [19]) is largely underexplored.

Since the landmark paper of Gupta and Kumar [5], substantial research has focused on analyzing wireless network capacity under various topologies and PHY layer technologies (*e.g.*, MIMO and directional antennas [20]). Existing analysis unanimously assumes half-duplex radios, and targets capacity scaling laws under infinite number of nodes. In this work, we have developed simple models to analyze the unique features of full-duplex networks, and derive the *capacity gain* over half-duplex networks.

The utility-optimal full-duplex MAC in this paper shares similar spirit with existing work on utility-optimal CSMA [6], [21]. However, our objective is not to implement a new MAC, but rather to perform a fair comparison between the optimal throughput of half- and full-duplex networks, thus distilling the key factors that future MAC protocols should take into account in order to explore the full-duplex gain.

VI. Conclusion

While it is tempting to believe that full-duplex can double wireless capacity, this paper disproves the perception through asymptotic analysis and network optimization. Indeed, for a single link, full-duplex may have a capacity gain of 2 over half-duplex, but in large-scale wireless networks, spatial reuse and asynchronous contention effects significantly undermine the actual benefits of full-duplex. Future network designers need to reengineer the MAC protocols taking into these two factors, in order to translate the PHY layer full-duplex gain into network layer throughput improvement.

For tractability, our analysis has made a number of assumptions. The analysis of full-duplex capacity gain in 2-D networks assumes an oracle scheduler that greedily enables bidirectional full-duplex transmissions. Whereas the utility-optimal MAC allows a mix of full-duplex and half-duplex transmissions, it adopts a randomized CSMA-style scheduler. As future work, we will derive the full-duplex capacity when an oracle, adaptive scheduler is used. In addition, consistent with the protocol model, we assumed perfect carrier sensing when comparing half- and full-duplex throughput under the utility-optimal MAC. Since practical MAC protocols still suffer from hidden- and exposed terminal problems, both half- and full-duplex networks may underutilize the capacity, possibly to different extent. It would be interesting to test the full-duplex gain under these practical conditions.

References

[1] J. I. Choi, M. Jain, K. Srinivasan, P. Levis, and S. Katti, "Achieving Single Channel, Full Duplex Wireless Communication," in *Proc. of ACM MobiCom*, 2010.
[2] M. Duarte, C. Dick, and A. Sabharwal, "Experiment-Driven Characterization of Full-Duplex Wireless Systems," *IEEE Transactions on Wireless Communications*, vol. 11, no. 12, 2012.
[3] Engadget, "Researchers demo full-duplex wireless: double the throughput with no new towers," Sep. 2011.
[4] Slashdot, "Full Duplex Wireless Tech Could Double Bandwidth," Sep. 2011.
[5] P. Gupta and P. Kumar, "The Capacity of Wireless Networks," *IEEE Transactions on Information Theory*, vol. 46, no. 2, 2000.
[6] J. Liu, Y. Yi, A. Proutiere, M. Chiang, and H. V. Poor, "Towards Utility-Optimal Random Access Without Message Passing," *Wirel. Commun. Mob. Comput.*, vol. 10, no. 1, 2010.
[7] J. Liu, D. Goeckel, and D. Towsley, "Bounds on the Gain of Network Coding and Broadcasting in Wireless Networks," in *Proc. of IEEE INFOCOM*, 2007.
[8] P. Kumar, "A Correction to the Proof of a Lemma in "The Capacity of Wireless Networks"," *IEEE Trans. on Information Theory*, 2003.
[9] M. Z. Brodsky and R. T. Morris, "In Defense of Wireless Carrier Sense," in *Proc. of ACM SIGCOMM*, 2009.
[10] S. Sen, R. Roy Choudhury, and S. Nelakuditi, "No Time to Countdown: Migrating Backoff to the Frequency Domain," in *ACM MobiCom*, 2011.
[11] IEEE, "802.11: Wireless LAN Medium Access Control (MAC) and Physical Layer (PHY) Specifications," 2007.
[12] M. Vutukuru, K. Jamieson, and H. Balakrishnan, "Harnessing Exposed Terminals in Wireless Networks," in *Proc. of USENIX NSDI*, 2008.
[13] L. Jiang and J. Walrand, "A Distributed CSMA Algorithm for Throughput and Utility Maximization in Wireless Networks," *IEEE/ACM Trans. Netw.*, vol. 18, no. 3, 2010.
[14] J. Andrews, R. Ganti, M. Haenggi, N. Jindal, and S. Weber, "A Primer on Spatial Modeling and Analysis in Wireless Networks," *IEEE Comm. Magazine*, vol. 48, no. 11, 2010.
[15] Conniq, "Duplexing Scheme in WiMAX: TDD or FDD," http://www.conniq.com/WiMAX/tdd-fdd.htm, 2012.
[16] A. Sahai, G. Patel, and A. Sabharwal, "Pushing the Limits of Full-duplex: Design and Real-time Implementation," *CoRR*, vol. abs/1107.0607, 2011.
[17] M. Duarte, A. Sabharwal, V. Aggarwal, R. Jana, K. K. Ramakrishnan, C. W. Rice, and N. K. Shankaranarayanan, "Design and Characterization of a Full-duplex Multi-Antenna System for WiFi networks," *CoRR*, vol. abs/1210.1639, 2012.
[18] X. Fang, D. Yang, and G. Xue, "Distributed Algorithms for Multipath Routing in Full-Duplex Wireless Networks," in *IEEE MASS*, 2011.
[19] M. Kodialam and T. Nandagopal, "Characterizing Achievable Rates in Multi-hop Wireless Mesh Networks with Orthogonal Channels," *IEEE/ACM Trans. Netw.*, vol. 13, no. 4, 2005.
[20] C. Jiang, Y. Shi, Y. Hou, W. Lou, S. Kompella, and S. Midkiff, "Toward Simple Criteria to Establish Capacity Scaling Laws for Wireless Networks," in *Proc. of IEEE INFOCOM*, 2012.
[21] B. Nardelli, J. Lee, K. Lee, Y. Yi, S. Chong, E. Knightly, and M. Chiang, "Experimental Evaluation of Optimal CSMA," in *IEEE INFOCOM*, 2011.